Cellular Oncology 26 (2004) 125–134
IOS Press

An automated method for the quantification and fractal analysis of immunostaining

Armin Gerger, Patrick Bergthaler and Josef Smolle *
Department of Dermatology, University of Graz, Austria

Received 17 October 2003
Accepted 22 March 2004

Abstract. *Aims*. In tissue counter analysis (TCA) digital images of complex histologic sections are dissected into elements of equal size and shape, and digital information comprising grey level, colour and texture features is calculated for each element. In this study we assessed the feasibility of TCA for the quantitative description of amount and also of distribution of immunostained material.

Methods. In a first step, our system was trained for differentiating between background and tissue on the one hand and between immunopositive and so-called other tissue on the other. In a second step, immunostained slides were automatically screened and the procedure was tested for the quantitative description of amount of cytokeratin (CK) and leukocyte common antigen (LCA) immunopositive structures. Additionally, fractal analysis was applied to all cases describing the architectural distribution of immunostained material.

Results. The procedure yielded reproducible assessments of the relative amounts of immunopositive tissue components when the number and percentage of CK and LCA stained structures was assessed. Furthermore, a reliable classification of immunopositive patterns was found by means of fractal dimensionality.

Conclusions. Tissue counter analysis combined with classification trees and fractal analysis is a fully automated and reproducible approach for the quantitative description in immunohistology.

Keywords: Image analysis, tissue counter analysis, quantification, fractal geometry, immunostaining

1. Introduction

There is a growing trend towards the objective quantification of immunohistochemical staining. Many studies dealing with automated quantification in immunohistochemistry show quite successful results in discriminating immunostained regions using dynamic threshold operations, color based classifiers or pixel-wise measurements [4,10,12,13]. However, fully automated discrimination of immunostained particles is a complex task, and semi-automated or even interactive measurements have to be performed [5,11]. Since structures in histologic sections are usually arranged in a complex pattern, simple threshold operations are often not sufficient for practical application in automated immunohistochemical analysis, though they are applied [18]. Consequently, interactive tracing of structures of interest has to be performed by the operator. This is subject to intra- and inter-personal variation and time-consuming user interaction is usually necessary. In contrast to conventional systems, tissue counter analysis (TCA), a recently developed and validated procedure, overcomes these problems since digital information is gathered from a series of tissue elements and significant measuring features are automatically selected by statistical approaches [14, 15]. By the method, a grid of measuring masks (elements) of equal size and shape is placed over histologic sections and the digital content of each element is automatically evaluated (Table 1). During a learning phase, digital information of each element comprising grey value, colour and texture features is stored together with the interactive user classification (e.g., background, immunopositive tissue elements, "other" tissue elements). Based on pooled data obtained from

*Corresponding author: Dr. Josef Smolle, Division of Analytic-Morphologic Dermatology, Department of Dermatology, University of Graz, Austria, Auenbruggerplatz 8, A-8036 Graz, Austria. Tel.: +43 316 385/2530; Fax: +43 316 385/2466; E-mail: josef.smolle@kfunigraz.ac.at.

these learning sets, one can grow a decision tree separating the various classes of elements. Once such a classification procedure is established, it can be implemented into an image analysis system and used for fully automated, user independent classification of tissue elements [16]. As described in previous studies, TCA serves as a potential tool in automated image analysis and works independently of the image source, since experiments not only at light and epiluminescence microscopic levels but also at the macroscopic level were equally successful [6–8]. In this study we tested our method on immunostained histologic sections of normal skin with antibodies against cytokeratin (CK) and leukocyte common antigen (LCA). At first, our system was trained for differentiating between background and tissue elements on one hand and between immunostained tissue and so-called other tissue elements on the other. In a second step, slides were automatically screened and the procedure was tested for the quantitative description of immunohistochemically stained structures. Additionally, fractal analysis using the box-counting method was applied to all cases describing the architectural distribution of immunostained material.

For fractal analysis, each tissue element labeled as positive in the TCA procedure was reduced to one pixel in a de-magnified binary image. Each of these pixels was regarded as a "point" from a geometric point of view, yielding a dimensionality of 0. Thus, a continuous line of positive pixels would represent a line with a dimensionality of 1, and a cluster of positive pixels would comprise an area with a dimensionality of 2. With the box counting method [1], arrangements of positive pixels at various scales are evaluated and a fractal dimensionality is estimated, which would be close to 0 when there is a dissemination of widely spaced single pixels, and close to 2, when large positive areas prevail.

2. Material and methods

2.1. Specimens

The specimens were randomly sampled from the Dermatopathology files of the Department of Dermatology, University of Graz, Austria. In total, 20 samples of clinically normal appearing skin taken from the uninvolved part of excision biopsies of melanocytic nevi were used. All biopsies were routinely formalin-fixed, embedded in paraffin and cut at a section thickness of 4 μm.

Table 1
Measurement features obtained for each element. For detailed information see [3] and [8]. Features which were crucial for differentiating between various classes of elements are highlighted (background versus tissue: italic; CK immunopositive versus "other" tissue elements: bold; LCA immunopositive versus "other" tissue elements: underlined)

Grey level features	Haralick texture features	Colour features
MEAND/grey	HARAM1	MEANDR/grey
STDD/grey	HARAM2	**MEANDG/grey**
SKEWD	HARAM3	**MEANDB/grey**
KURTD	HARAM4	STDDR/grey
ENERGYD	HARAM5	STDDG/grey
ENTROPYD/bit	**HARAM6**	STDDB/grey
MIND/grey	HARAM7	SKEWR
MAXD/grey	HARAM8	SKEWG
SUMD/grey	HARAM9	SKEWB
SUMQD/grey^2	HARAM10	KURTR
MOMENTDC20/pixel^2	HARAM11	KURTG
MOMENTDC11/pixel^2	HARAR1	KURTB
MOMENTDC02/pixel^2	HARAR2	ENERGYR
MOMENTDC30/pixel^3	HARAR3	ENERGYG
MOMENTDC21/pixel^3	HARAR4	ENERGYB
MOMENTDC12/pixel^3	HARAR5	ENTROPYR
MOMENTDC03/pixel^3	HARAR6	ENTROPYG
MOMENTDI1	HARAR7	ENTROPYB
	HARAR8	MINR
	HARAR9	MING
	HARAR10	MINB
	HARAR11	MAXR
		MAXG
		MAXB
		SUMR
		SUMG
		SUMB
		SUMQR
		SUMQG
		SUMQB

2.2. Immunohistochemistry

Highly sensitive immunohistochemistry was performed with an automated immunostainer (Horizon, DAKO A/S, Glostrup, Denmark) using an indirect streptavidin–biotin method following the standardized MSIPE-protocol of the provider (DAKO). Two different primary antibodies were applied: Mouse Anti-Human Cytokeratin against CK (clone MNF116, 1 : 25, DAKO) and Mouse Anti-Human CD45 against LCA (clone 2B11 + PD7/26, 1 : 50, DAKO). In brief, in nor-

mal tissue the CK antibody shows a broad pattern of reactivity with human epithelial tissues from simple glandular to stratified squamous epithelium, including epidermis, eccrine sweat glands, mammary gland ducts, tracheal epithelium and amniotic epithelium, whereas the LCA antibody labels lymphoid cells and to a variable degree macrophages and histiocytes. In each case, one section served as negative control by omission of the primary antibody.

2.3. Equipment and settings

Digital images were taken using an Axioskop 2 bright field microscope with a scanning table (Zeiss, Oberkochen, Germany) mounted with a CCD three-chip color video camera (Sony, Tokyo, Japan) connected to a KS 400 3.0 image analysis unit (Zeiss Vision, Hallbergmoos, Germany; [3]). A 20× objective was used with an image size of 764×573 pixels, yielding a pixel size of 0.65 μm. For each slide a white reference image was taken and smoothed with a 10×10 average filter. Illumination was set according to Köhler's principle and kept constant during the study. Image brightness and colour temperature were kept constant, with colour temperature being automatically adjusted to 3200 K by the Axioplan imaging software. Adjustment for brightness was performed with a set of neutral filters inserted into the illuminated beam. For each image, additive shading correction was performed.

2.4. Tissue counter analysis

In each slide, a measuring region was defined which included a whole section. For this purpose, the observer defines two points outside the lesion from which a rectangle is calculated serving as a border for further measuring procedures. When learning sets for background and tissue separation were created, in each histologic section random digits automatically selected 5 fields, and a lattice of 108 (12×9) measuring masks each was used for measurement within the images of 764×573 pixel size (Fig. 1). 20 instead of 5 fields using an identical grid of 108 masks were randomly selected when datasets differentiating immunopositive tissue and so-called other tissue elements were sampled. In the automated procedure, however, the whole measuring region was scanned and each field of vision was evaluated by a grid of 300 (20×15) measuring masks (Fig. 2A,B). The individual square measuring masks were of 32×32 pixels size. An image part covered by a measuring mask is called an element. For each element, 70 measuring parameters including grey level features, colour features and Haralick texture features were automatically assessed (Table 1; [3,9]). In learning procedures each element was interactively classified as belonging to background, immunopositive tissue or "other" tissue and classifications were stored together with the digital features into the SPSS-file for-

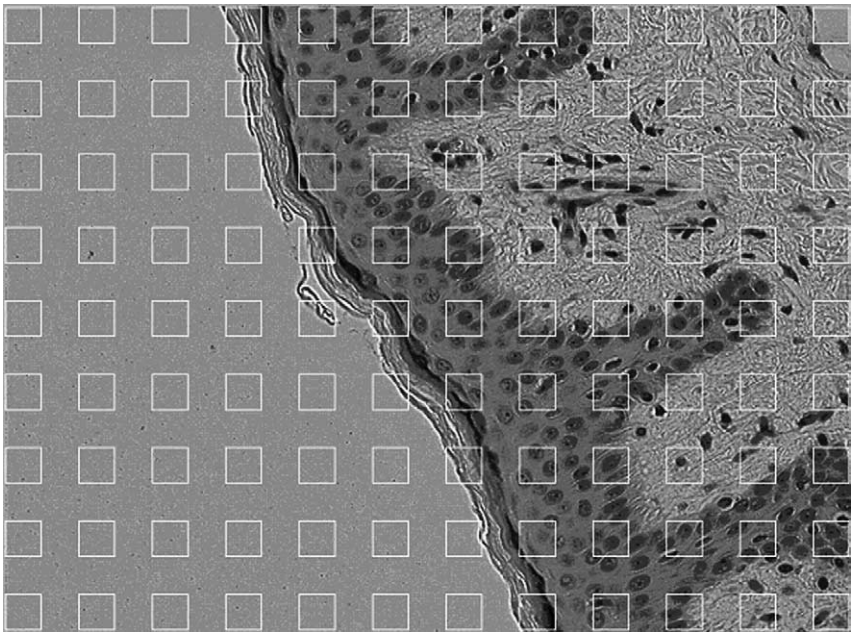

Fig. 1. A field of vision with measuring masks of equal size and shape during learning phases. Elements were interactively classified as belonging to background, tissue or immunostaining.

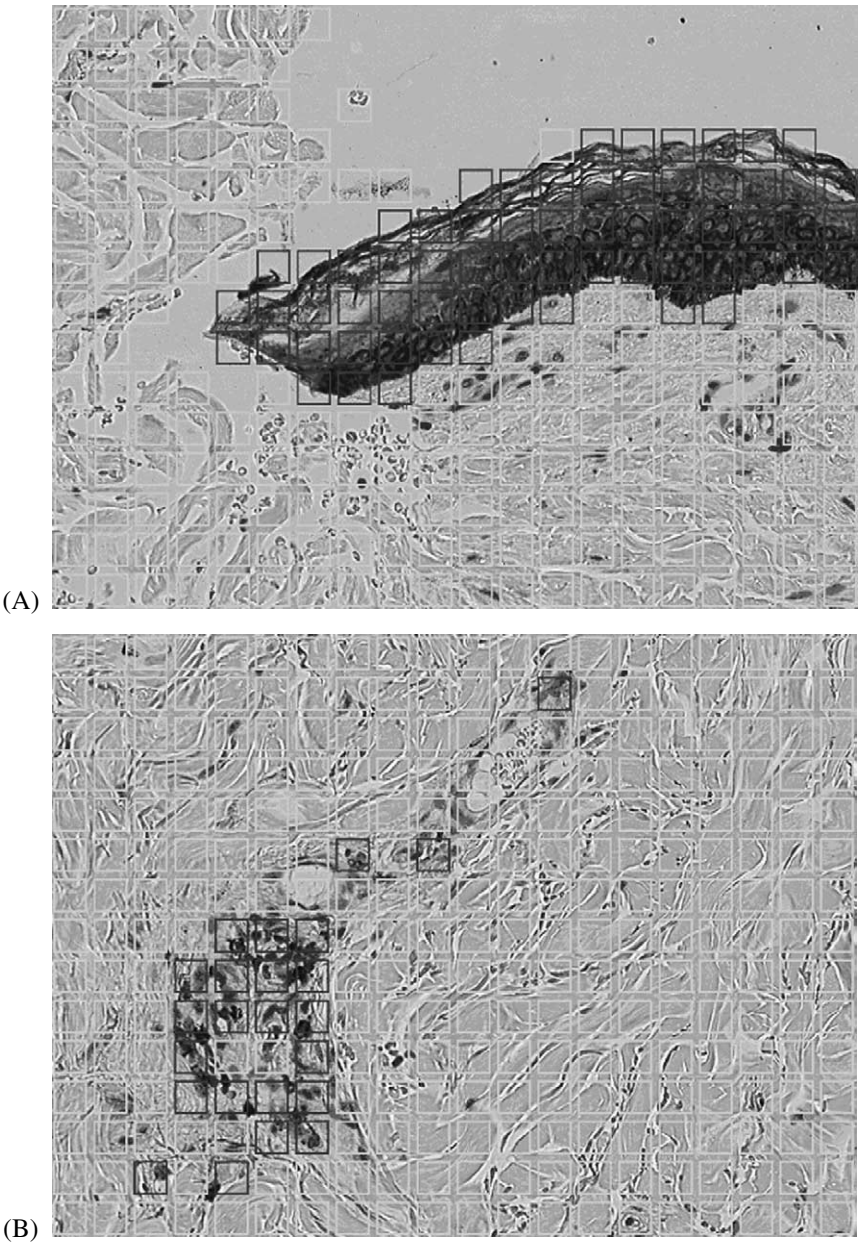

Fig. 2. (A): Example of CK stained slide. Background elements were automatically excluded and only immunopositive (black frames) and "other" tissue elements (grey frames) are highlighted. (B): Example of LCA stained slide. Note the clear-cut difference between immunopositive (black frames) and "other" tissue elements (grey frames).

mat. On these learning sets, classification and regression tree (CART) analysis was performed in order to obtain split-criteria (rules) for differentiating particular classes. In automated measuring procedures, the features measured in each element were tested for fulfilling certain rules. Based on these rules, the particular element was automatically assigned to a particular class.

2.5. CART

In our study we used the CART 4.0 software (Classification and Regression Tree; Salford Systems, San Diego, USA). CART is a decision-tree tool for data mining, predictive modeling and data preprocessing. The software automatically searches for important pattern and relationships even in highly complex data us-

ing the original CART code [2,17]. In the search for pattern in databases it is essential to avoid the trap of "over-fitting", or finding patterns that apply only to the training data. In CART, however, test disciplines are embedded, which ensure that the patterns found will hold up when applied to new data. For this purpose a total of 10 trees based on independent subsets of the learning sample are created. For each tree, CART begins by growing the maximal tree possible and then prunes those sections of the tree that contribute least to overall accuracy, pruning all the way back to the root node. A root node is the first node in a decision tree containing also the first split criterion, which leads to two daughter nodes. If the nodes cannot be divided anymore, they are designated as terminal nodes. Only the tree that performs best on its subsample is used for further analysis.

2.6. Fractal geometry

In addition to the classical task of assessing the "amount" of positively stained material in immunohistological slides, the distribution of the material could be of interest. Therefore we developed a method based on tissue counter analysis which describes the distribution by means of fractal analysis. A binary image showing the immunostained material of the whole section was created. For this purpose, each measuring mask labeled as positive for immunohistology was demagnified to a single positive pixel. One pixel of this de-magnified image corresponds to 20.8 μm. The binary image was overlayed with a regularly meshed lattice of square boxes of decreasing size covering always the whole image, with minimum size of the boxes being identical to single pixels in the de-magnified image. The number of boxes containing at least one immunohistologically positive element was counted and this number plotted against the box width. From the steepness of the regression line after log/log transformation the fractal dimensionality can be calculated as described by Baish and Jain [1] (Fig. 3A,B; [1]).

2.7. Data sets

For the task of differentiating between background and tissue elements, 5 cases in each group (CK, LCA, negative controls) were measured and interactively classified as mentioned above resulting in a learning set of 8100 elements (3287 background and 4813 tissue elements). CART analysis of the learning set provided a decision tree, which was used for the exclusion of background elements in further analysis. When only tissue elements were shown to the operator, 10 randomly selected cases in each group were evaluated. This time, the observer classified all elements as belonging to CK or LCA immunopositive tissue on one hand, or "other" tissue components on the other. Tissue elements derived from the negative controls were pooled either with tissue elements obtained from the CK stained slides (889 CK immunopositive and 27107 "other" tissue elements; overall 27996) or LCA stained slides (367 LCA immunopositive and 29572 "other" tissue elements; overall 29939) resulting in a learning set for each antibody. Classification trees based on

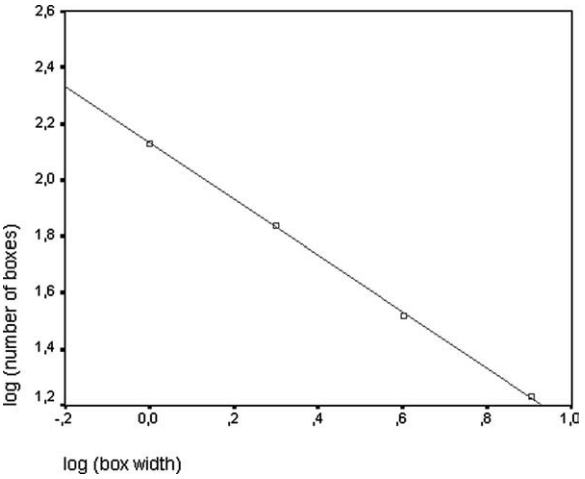

(A)

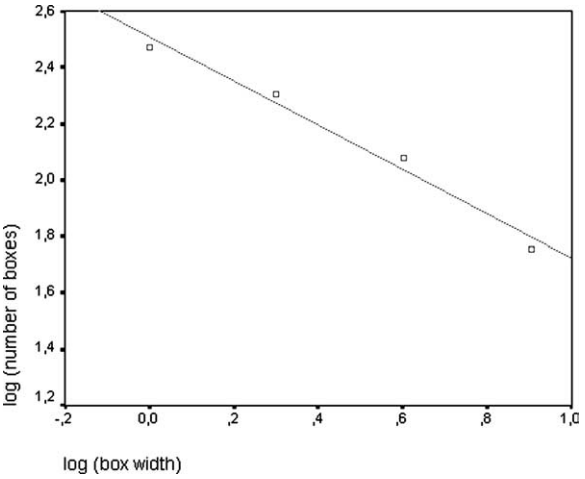

(B)

Fig. 3. (A): Log–log graph of box number versus box width for a sample of CK stained slides. The slope of the regression line indicates the box-counting fractal dimension (FD = 1.000000938). (B): Log–log graph for a sample of LCA stained slides (FD = 0.788844841).

the datasets were used for collecting either CK immunopositive or LCA immunopositive elements when a whole section was measured in each case.

2.8. Statistics

Basic statistics (mean, standard deviation), comparison of mean values (t-test) and correlation coefficient (Pearson) were performed using the SPSS statistical software package (SPSS Inc., Sunnyvale, USA). A p value of less than 0.01 was considered to indicate statistical significance. CART analyses were performed using the CART V4.0 software (Salford Systems, San Diego, USA).

3. Results

3.1. Classification of tissue elements

CART analysis of background versus tissue elements led to a correct classification of 98.0%. When the immunopositive components of the tissue elements were considered, CART analyses yielded to a correct classification of 97.0% of CK immunopositive elements and 88.9% of LCA immunopositive elements versus "other" tissue elements within the learning sets. Applied to the individual cases of immunostained slides using the generated decision trees, background elements were automatically excluded and only immunopositive (blue frames) and "other" tissue elements (grey frames) were shown to the operator and counted by the image analysis system when each field was measured (Fig. 2A,B). For highlighting the immunopositive architecture of each antibody in contrast to "other" tissue, de-magnified images displaying a scanning view of the whole section were generated (Fig. 4A,B,C; Fig. 5A,B,C). Each pixel in Fig. 4B,C and 5B,C corresponds to a measuring mask (32×32 pixel) as shown in Figs 1 and 2A,B.

Since CART performs automated feature selection within the set of grey level, colour and texture parameters for classification purposes, only a subset was finally incorporated in the particular classification trees. For the task of differentiating between background and tissue, it turned out that CART considered only one colour parameter, namely *ENTROPYG*, as necessary for high performance classification. Describing immunopositive tissue, which in fact is a more complex task, CART required a subset of 6 grey level, colour and texture features (*MEAND/grey,*

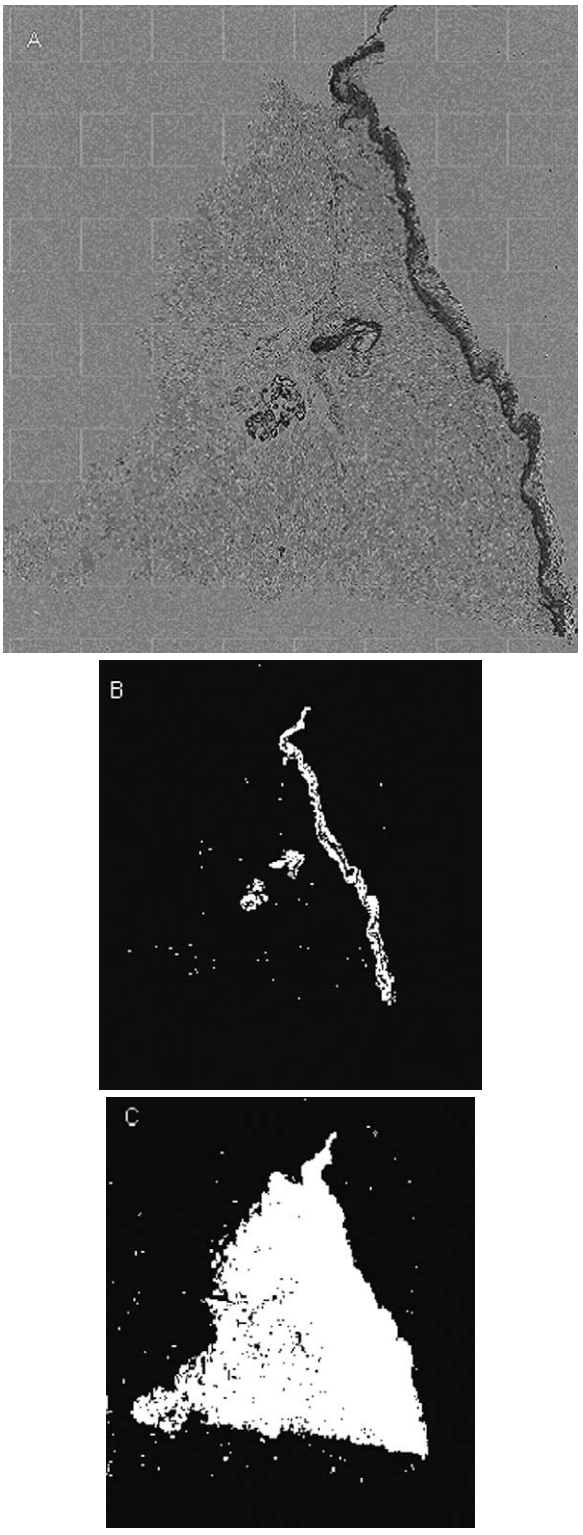

Fig. 4. De-magnified image of a CK stained tissue section (A). The architecture of immunopositive (B) and "other" tissue elements (C) is represented in monochrome images.

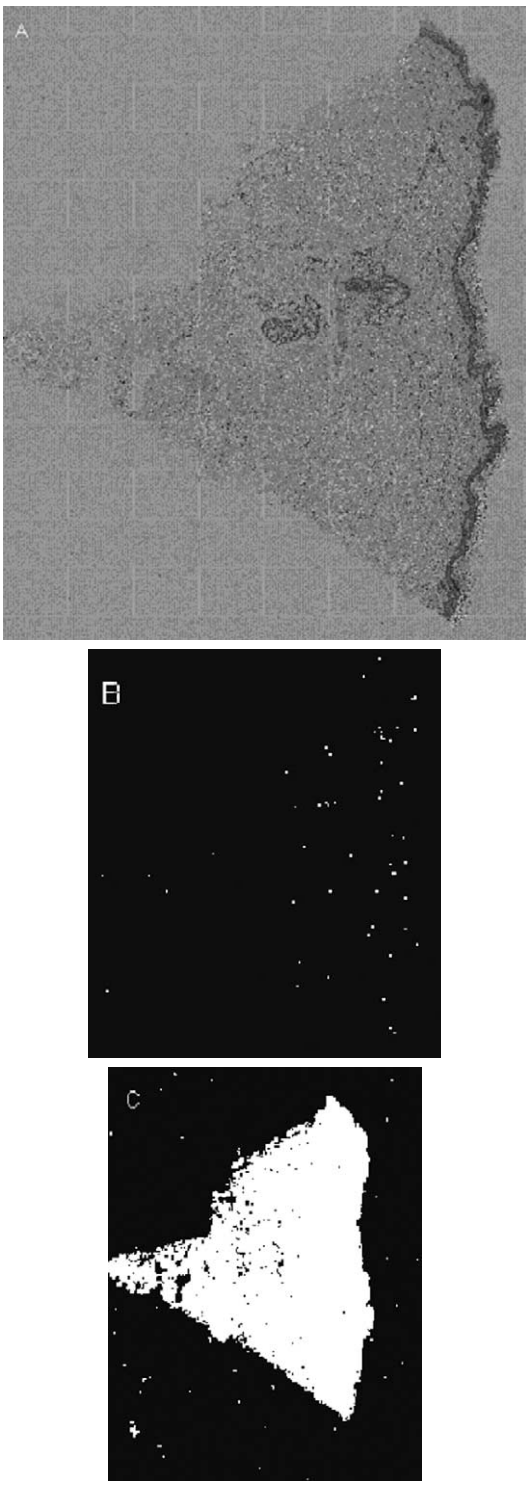

Fig. 5. De-magnified image of LCA immunostaing of an adjacent section of the same tissue as displayed in Fig. 4. Overview (A); Immunopositive architecture (B); Immunonegative architecture (C).

SUMQD/grey^2, HARAM6, MEANDG/grey, SUMQB and MEANDB/grey) for CK and 6 colour and texture features (*HARAM4, HARAM7, STDDG/grey, STDDB/grey, MING and MINB*) for LCA stained tissue classification (Table 1).

3.2. Quantitative description and fractal dimension

The relationship between the number and percentage of immunopositive elements, the number of tissue elements overall and the fractal dimension on the one hand and the type of antibody used on the other was evaluated. Within the set of immunostained cases no significant difference was found between the number of tissue elements in CK stained and LCA stained sections ($p = 0.129$). When the number and percentage of immunopositive elements were considered, 1979.4 ± 1536.0 ($5.9 \pm 5.2\%$) elements were found in CK stained sections in contrast to 283.7 ± 342.5 ($1.0 \pm 1.2\%$) elements in LCA stained sections. T-test of the number and percentage of immunopositive elements revealed a significant difference between both antibodies ($p < 0.001$; Fig. 6).

Evaluating the fractal geometry of each antibody, CK stained slides yielded a fractal dimension of 1.2 ± 0.1, whereas LCA stained slides produced a dimension of 0.4 ± 0.2 ($p < 0.001$; Fig. 7). This is in agreement with the biological distribution of the immunostained structures: Cytokeratins, as a component of epithelial cells, are limited to a certain anatomic compartment which appears as a broad linear structure in the tissue section. Leukocytes, in contrast, are often dispersed in the interstitial connective tissue, yielding individually spaced elements and small groups.

3.3. Reproducibility of CK and LCA counts

To test the reproducibility of our system, 10 cases (5 CK and 5 LCA) were measured twice at an interval of several weeks. Correlation between the measurements were $r = 0.999$ and $r = 0.980$ for the percentage and fractal dimension of immunopositive tissue elements and $r = 1.00$ for the number of the total of all tissue elements.

3.4. Time requirement

Depending on the size of the section, in particular the number of fields measured in each slide, automated measurements take 5 to 40 minutes. User interaction is limited to defining the corners of a rectangular measuring region which should include the whole histologic section. This task, however, takes about only 1 minute.

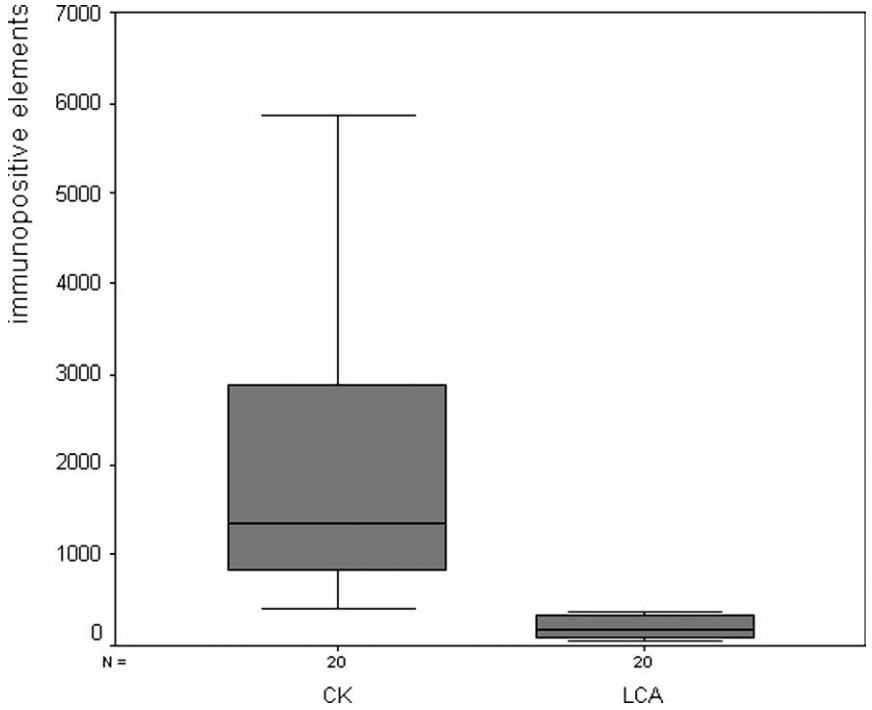

Fig. 6. Boxplot of the number of immunopositive tissue elements found in CK and LCA stained sections (t-test: $p < 0.001$).

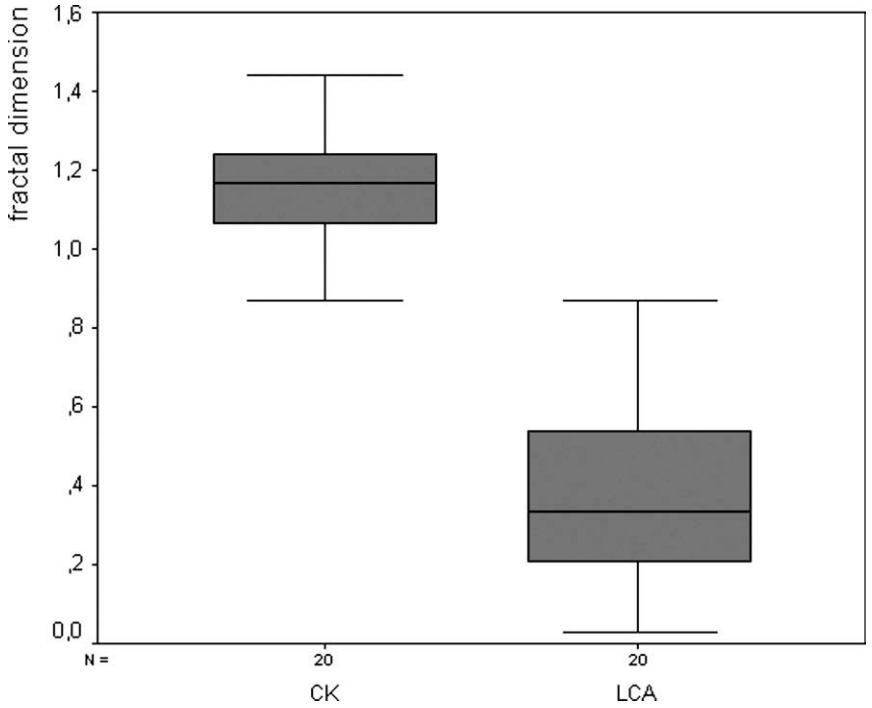

Fig. 7. Boxplot of the fractal dimension of immunopositive tissue elements found in CK and LCA stained sections (t-test: $p < 0.001$).

4. Discussion

We have described here an approach that allows fully automated quantification of immunohistology. Besides the amount of tissue of interest, which is most often the solely output of other methods, TCA and CART additionally enable description of the spatial distribution by means of fractal analysis.

By the method, digital images of tissue scenes are divided into elements of equal size and shape and features are calculated by extracting the digital information in each square element. In learning phases, thousands of elements have to be interactively classified by an operator as belonging to particular classes of tissue components. This task, however, has only been done once, since CART analysis, applied to the created learning sets, defines rules for classification of new elements. The software turned out to be a powerful and reliable classification tool so that we needed only one type of classification algorithm in the whole study. Arbitrary feature selection among the overall 70 measuring parameters provided by our image analysis software was not necessary, since CART independently performs the selection of significant measuring parameters. Within the whole set of features measured automatically by the KS 400 image analysis unit, it turned out that not only grey level and colour, but also texture features were selected by CART for classification procedures. By reproducing the interactive classifications, accuracy of about 90–100% was achieved by the algorithm.

In contrast to a conventional image analysis procedure based on single pixels, TCA shows the advantage that digital information not of individual pixels, but of a region can be taken into account. Therefore, not only the three grey values of the three colour channels can be taken into account, but also parameters concerning histogram moments and texture. By this approach, classification procedures can be based on a broader range of information than conventional pixel-by-pixel methods.

This fact is underlined by the findings obtained in the discrimination between tissue and background: Though a single parameter has turned out to be sufficient according to the CART procedure, it was not a simple grey value of a particular colour channel as it might have been found in pixel-by-pixel analysis, but the entropy of the green channel histogram.

Applied to whole slides of immunostained tissue scenes, our system detected automatically CK and LCA immunopositive tissue. User interaction was limited by defining a rectangular measuring region including the whole histologic section. This task, however, takes about one minute. To evaluate the recognition process, immunopositive tissue elements were shown to the operator by blue frames and counted by the image analysis system. Classification results visualized on the computer screen were in good agreement with visual control by the observer. When the number and percentage of CK and LCA immunopositive tissue was statistically evaluated, high reproducibility of the amount of stained tissue resulted.

Besides amount of tissue, distribution may be important and may differ between various immunohistological structures. Since TCA already produces a pattern of "boxes", our approach seemed to be particularly suitable to the fractal analysis method described by Baish and Jain [1]. They previously used fractal geometry to consider the fractal dimension of vascular patterns in tumors. Applied to staining patterns in normal skin, we tested the method for describing the distribution of CK and LCA immunopositive elements. Compact areas for CK with small clusters of sweat glands showed a dimensionality between "line" and "area", i.e. between 1.0 and 2.0 whereas dissemination of inflammatory cells, individual cells and small clusters represents a dimensionality between "point" and "line", i.e. between 0.0 and 1.0. This rather low value of fractal dimensionality is due to the fact that in the de-magnified measurement images a small amount of positive material is de-magnified to a single pixel, and that single pixels are considered as "points" in terms of geometry. It turned out, that clear classification between CK and LCA patterns by means of fractal dimension can be achieved.

There are, however, several limitations to be addressed before tissue counter analysis can be proposed as a practical tool in routine immunohistochemical settings. All specimens have been prepared in the same laboratory with a standard staining protocol. Greater variations in the histotechnical procedure would definitely hamper the final results. Furthermore, the settings of the digital camera, microscope and image analysis unit had to be kept constant in order to avoid conflicting results.

In the future, tissue counter analysis (TCA) combined with classification and regression trees (CART) and fractal analysis will be tested on a wider selection of specimens and pathologic conditions. Especially, the significance of fractal dimensionality should be determined in further work.

In conclusion, our study shows that tissue counter analysis is a fully automated and reproducible ap-

proach for the quantitative description of amount and also of distribution of immunopositive structures in immunohistology.

Acknowledgement

The study was supported by the "Jubiläumsfonds der Österreichischen Nationalbank", project number 9297.

References

[1] J.W. Baish and R.K. Jain, Fractals and cancer, *Cancer Res.* **60**(14) (2000), 3683–3688.

[2] L. Breiman, J. Friedman, R. Olshen et al., *Classification and Regression Trees*, Pacific Grove, Wadsworth, 1984.

[3] Carl Zeiss Vision, KS 400 Imaging system, Release 3.0, Carl Zeiss Vision, Munich, 1997.

[4] G.A. Cecchi, S. Ribeiro, C.V. Mello and M.O. Magnasco, An automated system for the mapping and quantitative analysis of immunocytochemistry of an inducible nuclear protein, *J. Neurosci. Methods* **87**(2) (1999), 147–58.

[5] P.N. Furness, L. Rogers-Wheatley and K.P. Harris, Semiautomatic quantitation of macrophages in human renal biopsy specimens in proteinuric states, *J. Clin. Pathol.* **50**(2) (1997), 118–122.

[6] A. Gerger and J. Smolle, Diagnostic imaging of melanocytic skin tumors, *J. Cutan. Pathol*. **30** (2003), 247–252.

[7] A. Gerger and J. Smolle, Diagnostic tissue elements in melanocytic skin tumors in automated image analysis, *Am. J. Dermatopathol.* **25**(2) (2003), 100–106.

[8] A. Gerger, W. Sterry, R. Pompl and J. Smolle, Automated epiluminescence microscopy – tissue counter analysis using CART and 1-NN in the diagnosis of melanoma, *Skin. Res. Technol.* **9**(2) (2003), 105–110.

[9] R.M. Haralick, Textural features from image classification, *IEEE Trans. Syst. Man. Cypern.* **6** (1973), 619.

[10] P. Kiehl, K. Falkenberg, M. Vogelbruch and A. Kapp, Tissue eosinophilia in acute and chronic atopic dermatitis: a morphometric approach using quantitative image analysis of immunostaining, *Br. J. Dermatol.* **145**(5) (2001), 720–729.

[11] M. Klencki, D. Slowinska-Klencka and A. Lewinsk, Multifarious system for quantitative analysis of histologic compartments, *Comput. Biomed. Res.* **30** (1997), 165–169.

[12] P. Ranefall, K. Wester, A.C. Andersson, C. Busch and E. Bengtsson, Automatic quantification of immunohistochemically stained cell nuclei based on standard reference cells, *Anal. Cell. Pathol.* **17**(2) (1998), 111–123.

[13] P. Ranefall, K. Wester and E. Bengtsson, Automatic quantification of immunohistochemically stained cell nuclei using unsupervised image analysis, *Anal. Cell. Pathol.* **16**(1) (1998), 29–43.

[14] J. Smolle, Computer recognition of skin structures using discriminant and cluster analysis, *Skin. Res. Technol.* **6** (2000), 58–63.

[15] J. Smolle, Diagnostic assessment of cutaneous melanoma and common nevi using tissue counter analysis, *Analyt. Quant. Cytol. Histol.* **22** (2000), 299–306.

[16] J. Smolle and A. Gerger, Tissue counter analysis of tissue components in skin biopsies – Evaluation using CART (Classification and Regression Tree), *Am. J. Dermatopathol.* **25**(3) (2003), 215–22.

[17] D. Steinberg and P. Colla, CART: *Tree-Structured Nonparametric Data Analysis*, Salford Systems, San Diego, 1995.

[18] F. Willemse, M. Nap, S.C. Henzen-Logmans and H.F. Eggink, Quantification of area percentage of immunohistochemical staining by true color image analysis with application of fixed thresholds, *Anal. Quant. Cytol. Histol.* **16**(5) (1994), 357–364.